High-Frequency, Magnetic-Field-Responsive Drug Release from Magnetic Nanoparticle/Organic Hybrid Based on Hyperthermic Effect

Koichiro Hayashi,[†] Kenji Ono,[‡] Hiromi Suzuki,[‡] Makoto Sawada,[‡] Makoto Moriya,[†] Wataru Sakamoto,[†] and Toshinobu Yogo*[,†]

Division of Nanomaterials Science, EcoTopia Science Institute, Nagoya University, Furo-cho, Chikusa-ku, Nagoya, 464-8603, Japan, and Department of Brain Function, Research Institute of Environmental Medicine, Nagoya University, Furo-cho, Chikusa-ku, Nagoya, 464-8601, Japan

ABSTRACT Magnetic nanoparticles (MNPs) generate heat when a high-frequency magnetic field (HFMF) is applied to them. Induction heat is useful not only for hyperthermia treatment but also as a driving force for drug-release. β-Cyclodextrin (CD) can act as drug container because of its inclusion properties. Drugs incorporated in the CD can thus be released through the use of induction heating, or hyperthermic effects, by applying a HFMF. In this study, we have synthesized folic acid (FA) and CD-functionalized superparamagnetic iron oxide nanoparticles, FA-CD-SPIONs, by chemically modifying SPIONs derived from iron(III) allylacetylacetonate. FA is well-known as a targeting ligand for breast cancer tumor and endows the SPIONs with cancer-targeting capability. Immobilization of FA and CD on spinel iron oxide nanoparticles was confirmed by Fourier transform IR (FTIR) and X-ray photoelectron spectroscopy (XPS). The FA-CD-SPIONs have a hydrodynamic diameter of 12.4 nm and prolonged stability in water. They are superparamagnetic with a magnetization of 51 emu g^{-1} at 16 kOe. They generate heat when an alternating current (AC) magnetic field is applied to them and have a specific absorption rate (SAR) of 132 W g^{-1} at 230 kHz and 100 Oe. Induction heating triggers drug release from the CD cavity on the particle - a behavior that is controlled by switching the HFMF on and off. The FA-CD-SPIONs are noncytotoxic for cells. Thus, FA-CD-SPIONs can serve as a novel device for performing drug delivery and hyperthermia simultaneously.

KEYWORDS: nanoparticle • magnetic properties • induction heating • drug release

1. INTRODUCTION

Magnetic nanoparticles (MNPs) exhibit unique properties such as induction heating under the application of high-frequency magnetic fields (HFMF) (1) and magnetic guidance (2), and therefore, can be incorporated into devices for magnetic hyperthermia (3), use in drug delivery systems (DDS) (4), and in magnetic resonance imaging (MRI) (5). MNPs accumulated in a tumor can act as hyperthermia-inducing agents, using the exothermic properties derived from hysteresis and/or Néel relaxation losses by application of HFMF (3) to raise the local temperature around cells. For these applications, MNPs are required to have a functionalized surface with biocompatible organic molecules, tumor-targeting ligands, or anticancer drugs.

Typical examples of DDS using MNPs are MNPs with biodegradable polymers that have drug inside them (6), and drug-immobilized MNPs via bond subjected to hydrolysis (7), which passively release drugs through the degradation of the polymer. Active release of the drug can be achieved using the volume change of drug carrier, which includes MNPs/thermosensitive polymer core/shell nanoparticles, by temperature and pH control (8−14). Also, static and oscillating magnetic field can act as external stimuli for drug release (15, 16). Misra et al. reported that the drug release rate is significantly enhanced in the presence of a magnetic field because of the pulsatile mechanical deformation that generates compressive and tensile stresses. In addition, the induction heating of MNPs under HFMF, or hyperthermic effect, triggers drug release. HFMF is quite useful as external stimulus because it is less-invasive than other methods and has a high-permeability in relation to the human body and can be operated remotely. Gu et al. combined the HFMF with photodynamic therapy to synthesize a potential candidate for bimodal therapy (17). Past reports on HFMF-responsive DDS utilized the collapse (18, 19) or the volume transition (20) of drug carriers as a means of releasing the drug. However, collapse of composite MNPs does not permit control of time interval and amount. Also, the drug release via the volume transition of the drug carrier requires heating composite MNPs above the proper temperature for hyperthermia (42−45 °C).

β-Cyclodextrin (CD) is a remarkable drug container due to its inclusion properties (21, 22). CD consists of seven D-glucopyranose residues linked by α-1,4 glycosidic bonds into a macrocycle whose cavity has an inner diameter of 7−8 Å. Because the inner cavity is hydrophobic and the outside is hydrophilic, CD can facilitate the incorporation of hydrophobic drugs into the cavity, thereby making drugs hydrophilic. Because the interaction between the drug and the CD is hydrophobic, the drug is not bound chemically to

* Corresponding author. E-mail: yogo@esi.nagoya-u.ac.jp.
Received for review March 18, 2010 and accepted June 13, 2010
[†] EcoTopia Science Institute, Nagoya University.
[‡] Research Institute of Environmental Medicine, Nagoya University.
DOI: 10.1021/am100237p

Scheme 1. Synthesis Procedure of FA-CD-SPIONs

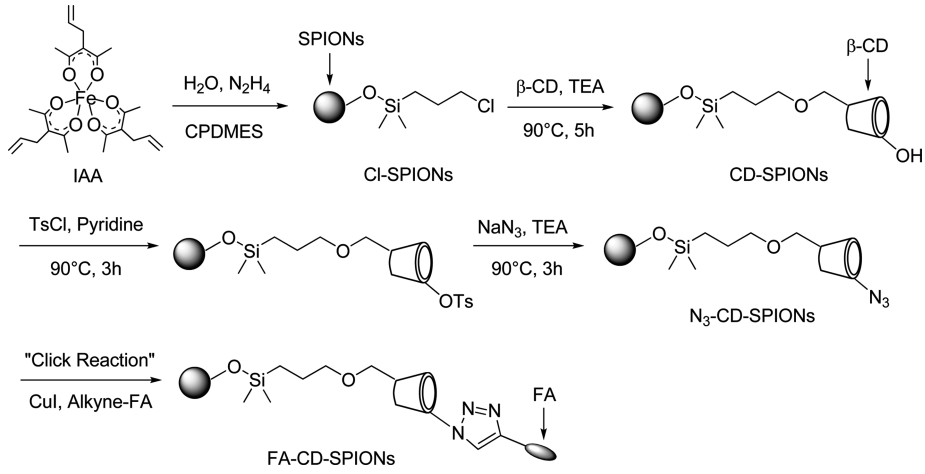

the CD. For this reason, the drug can be released from the cavity by depressing the hydrophobic interaction and accelerating diffusion, both of which are caused by hyperthermic action through the application of a HFMF. Furthermore, controlling the temperature under a HFMF to within 42−45 °C enhances the effect of the drug and allows hyperthermia treatment to occur at the same time.

Magnetic guidance is one of strategies for the accumulation of MNPs and drugs in an affected area. To accomplish more effective accumulation, the application of biological recognition mechanism is useful. For example, the α-COOH of folic acid (FA) specifically binds to folate receptors (FRs) overexpressed in breast cancer tumors (23−27), and therefore, FA-modified MNPs without the loss of α-COOH can selectively target tumors. We have succeeded in chemoselective modification of MNPs with FA through the application of alkyne−azide click chemistry (28).

This paper describes the synthesis of superparamagnetic iron oxide nanoparticles (SPIONs) modified with CD and FA. Moreover, we loaded tamoxifen (TMX), an anticancer drug used to treat breast cancer tumors, into CD on the SPIONs using the inclusion property of CD. Following the temperature control of the FA and CD-modified SPIONs under a HFMF at an optimum temperature for hyperthermia, we controlled the release of TMX by on−off switching of the field.

2. EXPERIMENTAL SECTION

Materials. Iron(III) allylacetylacetonate (IAA) was prepared as described in the literature (29). Ethanol (Kishida Chemical, Japan) was dried over magnesium ethoxide and then distilled before use. The following materials were used as received: hydrazine monohydrate ($N_2H_4 \cdot H_2O$, Tokyo Kasei, Japan), cuprous iodide (CuI, Wako Pure Chemical, Japan), sodium azide (NaN_3, Kishida Chemical, Japan), ammonium chloride (NH_4Cl, Kishida Chemical, Japan), 3-chloropropyldimethylethoxysilane (CPDMES, Gelest, USA), triethylamine (TEA, Wako Pure Chemical, Japan), p-toluenesulfonyl chloride (TsCl, Kishida Chemical, Japan), pyridine (Kishida Chemical, Japan), tamoxifen citrate (TMX, Wako Pure Chemical, Japan), and β-cyclodextrin (CD, Kishida Chemical, Japan). Alkyne-bound FA (alkyne-FA) for the click reaction was prepared according to our previous work (28).

Synthesis of SPIONs. The procedure for synthesis of SPIONs is as reported: hydrolysis and condensation of IAA (28, 30). The process allows easy organic modification of the resultant particles in the next stage. IAA (2.0 g, 4.26 mmol) was dissolved in ethanol (40 mL). $N_2H_4 \cdot H_2O$ (0.84 mL, 17.0 mmol), which serves as a reducing agent and pH adjuster, and water (7.36 g, 0.41 mol) dissolved in ethanol (10 mL) were injected into the precursor solution at 80 °C. The reaction mixture was refluxed for 15 h to obtain a black suspension, which was cooled to room temperature.

Synthesis of Cl-Functionalized SPIONs (Cl-SPIONs). CPDMES (3.06 g, 17.0 mmol) was added to the as-synthesized suspension with stirring, and the suspension was stirred at room temperature for 15 h (Scheme 1) (3). Removal of solvent followed by drying under a vacuum at room temperature yielded a black solid product. The product was washed five times with ethanol and dried under a vacuum at room temperature.

Synthesis of CD-Modified SPIONs (CD-SPIONs). CD was reacted with Cl on Cl-SPIONs as described in the literature (31). CD (1.80 g, 1.58 mmol) and TEA (0.16 g, 1.58 mmol) were dissolved in pyridine (30 mL). As-synthesized Cl-SPIONs (400 mg) were added to the solution under sonication to yield a black suspension (Scheme 1). The suspension was stirred at 90 °C for 5 h to eliminate chlorine (32). Black particles were collected from the suspension by magnet and washed 10 times with water. The products were dried under a vacuum at room temperature.

Synthesis of N_3-CD-Modified SPIONs (N_3−CD-SPIONs) for Click Reaction. Azidation of CD on SPIONs was carried out as described in the literature (31). As-synthesized CD-SPIONs (300 mg) were dispersed in a solution of TsCl (250 mg, 1.31 mmol) and pyridine (40 mL) using sonication, yielding a black suspension. The suspension was heated at 90 °C for 3 h (Scheme 1). NaN_3 (84 mg, 1.29 mmol) and TEA (130 mg, 1.28 mmol) were added and the suspension was heated at 90 °C for 3 h. The resultants were collected from the suspension by magnet and washed 10 times with water and ethanol. Finally, the products were dried under a vacuum at room temperature.

Synthesis of FA and CD-Modified SPIONs by Click Reaction (FA-CD-SPIONs). As-synthesized N_3-CD-SPIONs (200 mg) were dispersed in water (20 mL) by sonication to form a black suspension. CuI (3.9 mg) and alkyne-FA (200 mg) were dissolved in water (20 mL) and added. The suspension was heated at 70 °C for 1 h (33). The resultants were collected from the suspension using a magnet and washed 10 times with water. The products were dried under a vacuum at room temperature.

Structural Analysis. The IR spectra of IAA, Cl-SPIONs, CD-SPIONs, CD, N_3-CD-SPIONs, alkyne-FA, and FA-CD-SPIONs were obtained using a FTIR spectrometer (Nicolet, Nexus 470, Madison, WI). The organics of FA-CD-SPIONs was measured by

differential thermal analysis-thermogravimetry (DTA-TG, Rigaku, TG8120, Tokyo, Japan). Crystalline phases were analyzed by X-ray diffraction (XRD) using CuKα radiation with a monochromator (Rigaku, RINT-2500). Crystallite size was estimated using the 311 reflection of spinel iron oxide based upon the Scherrer equation. FA-CD-SPIONs were analyzed by X-ray photoelectron spectroscopy using Al Kα (1486.6 eV) radiation (XPS, Shimadzu, ESCA-3300, Kyoto, Japan). Peak deconvolution was carried out using the software supplied by the manufacturer. FA-CD-SPIONs were observed by transmission electron microscopy (TEM, Hitachi, H-800, Japan). The hydrodynamic diameter of FA-CD-SPIONs was measured by dynamic light scattering (DLS, Nikkiso, UPA-150, Tokyo, Japan).

Magnetic Properties. The magnetic properties of FA-CD-SPIONs were measured with a vibration sample magnetometer (VSM, Toei, VSM-5-15, Japan).

Hyperthermia Experiments. Hyperthermia experiments were performed by a method similar to that reported previously (28, 30). Temperature was measured as a function of time using a platinel thermocouple under a HFMF generated by a transistor inverter (230 kHz) with field coils (ϕ 120 × 5 turns). FA-CD-SPIONs powder (5.8 mg) was stuffed into a Teflon tube (ϕ 2.5 × 10 mm), and the tube was placed in the coil (230 kHz and 50−100 Oe). A thermocouple was inserted directly into the powder. Temperature evolution in a spherical phantom (ϕ 20 mm) dispersed with FA-CD-SPIONs powder was measured in the same way to estimate heating properties in a body. The phantom consisted of agar (4%), sodium chloride(0.24%), sodium azide (0.1%), and water (95.66%), thus resembling human tissues. FA-CD-SPIONs powder dispersed in water was mixed with agar, NaCl, and NaN_3 at the above ratio for preparation of simulated tissue. The mass of the powder per milliliter of phantom was 6.0 mg.

Preparation of TMX-Loaded FA-CD-SPIONs. FA-CD-SPIONs (150 mg) were placed in a vial containing TMX (20 mg, 3.55×10^{-5} mol), a hydrophobic drug, in water (50 mL). The mixture was stirred at room temperature for 72 h. TMX-loaded FA-CD-SPIONs were collected by magnet and dried under a vacuum overnight to yield 158.8 mg of product. For the drug-release experiment, two sets of suspensions were prepared from TMX-loaded FA-CD-SPIONs (10 mg) and water (20 mL).

TMX Release from FA-CD-SPIONs by Direct Heating. Prepared suspensions were maintained at 37 or 45 °C for 12 h using a constant-temperature bath. The concentration of TMX released from the FA-CD-SPIONs was monitored for absorption at 234 nm during a given time interval by UV−vis spectrophotometry (Jasco, V-570, Tokyo, Japan).

HFMF-Responsive TMX Release from FA-CD-SPIONs. To investigate how TMX release responded with hyperthermic action by applying a HFMF field, a suspension of TMX-loaded FA-CD-SPIONs (100 mg) and water (5 mL) was put under a HFMF field (230 kHz, 100 Oe) for 10 min. The temperature of the suspension was ~42.5 °C during this time. The suspension was then placed in a constant-temperature bath at 37 °C. These treatments−application of the field for 10 min followed by maintenance at 37 °C for 10 min−were repeated. The concentration of TMX released from the FA-CD-SPIONs by hyperthermic action was monitored by UV−vis spectrophotometry at a wavelength of 234 nm. The release amount of TMX was analyzed from the weight change of the FA-CD-SPIONs.

Cytotoxicity Assay and Cellular Uptake. Murine microglial cells were maintained in Eagle's MEM supplemented with 10% fetal calf serum, 5 mg/mL bovine insulin, 0.2% glucose, and 1 ng/mL murine granulocyte-macrophage colony-stimulating factor (G0282; Sigma-Aldrich), as described previously (34). The cells were seeded at 2×10^5 cells in a 6 cm plastic dish with a medium. The cytotoxicity of FA-CD-SPIONs was evaluated by determining the viability of microglial cells after incubation with the medium containing FA-CD-SPIONs (1−100 μg mL^{-1}) for 0.5 to 24 h. Cell viability test was carried out using WST assay. Furthermore, the cellular uptake of FA-CD-SPIONs was investigated by incubating microglial cells with the FA-CD-SPIONs in serum-containing media for 1 h. The FA-CD-SPIONs internalized by microglial cells were stained using Berlin blue. Cells were fixed with ethanol at room temperature for 10 min, washed with PBS three times, then incubated in mixture of 2% potassium ferrocyanide solution with 1% HCl in equal amounts for 20 min at room temperature and counterstained with Kernechtrot solution (Muto Pure Chemicals Co. Ltd., Tokyo, Japan). The cellular uptake of the FA-CD-SPIONs by glioma cells (GL 261) was investigated in a similar way.

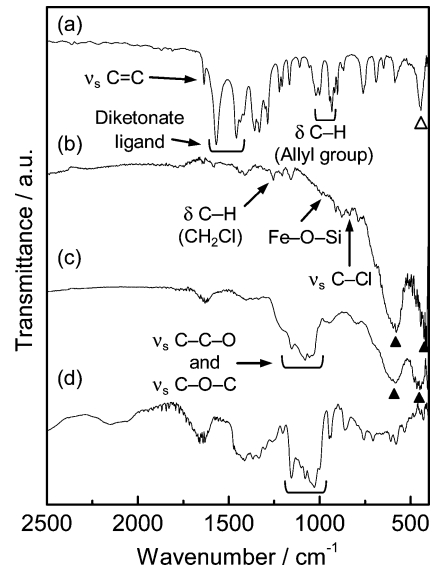

FIGURE 1. FTIR spectra of (a) IAA, (b) Cl-SPIONs, (c) CD-SPIONs, and (d) CD.

3. RESULTS AND DISCUSSION

Synthesis of FA-CD-SPIONs. SPIONs were synthesized by hydrolysis and condensation of IAA, and then CPDMES was added to the suspension at room temperature (Scheme 1). It is known that the surface of iron oxide synthesized by hydrolysis and condensation has a number of hydroxyl groups (Fe−OH), which react with Si−OH to form Fe−O−Si bonds (3). CPDMES was hydrolyzed by water in the suspension under basic conditions to form Si−OH bonds followed by formation of Fe−O−Si bonds through dehydration and condensation between the Si−OH and Fe−OH on the SPIONs. As a result, the 3-chloropropylsilyl group was immobilized on the surface of the SPIONs by the Fe−O−Si bonds to yield Cl-SPIONs. When CD was added to Cl-SPIONs and heated at 90 °C for 5 h, the Cl-SPION chloride underwent a nucleophilic substitution with the CD hydroxyl groups, resulting in formation of CD-SPIONs (32). Next, the CD hydroxyl groups were converted into tosyl groups with good leaving properties, which were substituted with azide groups by addition of NaN_3 at 90 °C for 3 h, yielding N_3-SPIONs (31). Finally, FA-CD-SPIONs were synthesized by click reaction between N_3-CD-SPIONs and separately synthesized alkyne-FA (28).

Figure 1 shows FTIR spectra for IAA, Cl-SPIONs, CD-SPIONs, and CD. IAA absorption bands at 1570, 1455, 1440, and 1415 cm^{-1} are due to the coordinated diketonate ligand (Figure 1a) (35). The band at 445 cm^{-1} marked with an open

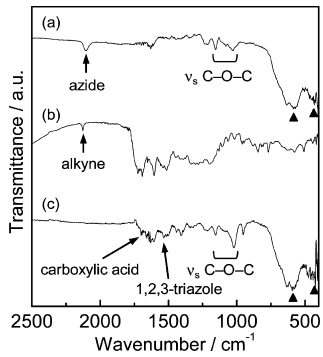

FIGURE 2. FTIR spectra of (a) N_3-CD-SPIONs, (b) alkyne-FA, and (c) FA-CD-SPIONs.

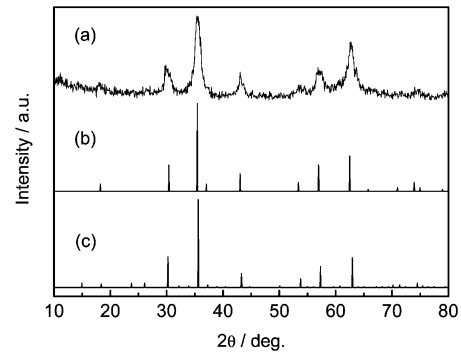

FIGURE 3. XRD patterns of (a) FA-CD-SPIONs, (b) Fe_3O_4, and (c) γ-Fe_2O_3.

triangle is due to the Fe−O bond. The band at 1635 cm^{-1} is due to the stretching vibration of C═C in the allyl group. Bands around 995, 940, 930, 915, and 900 cm^{-1} are due to bending vibrations of terminal C−H in the allyl group. After hydrolysis of IAA followed by reaction with CPDMES, an absorption band in the product at 964 cm^{-1} is due to the Fe−O−Si bond (Figure 1b) (36). Bands at 835 and 1258 cm^{-1} are due to C−Cl stretching vibration and C−H bending vibration in CH_2Cl, respectively. Bands at 585 and 453 cm^{-1} marked with solid triangles are due to Fe−O bonds in spinel (37). After modification with CD, the spectrum for CD-SPIONs shows that the bands attributed to CH_2Cl disappear and new bands appear between 1260 and 1000 cm^{-1} due to C−O−C stretching vibration in ether and C−C−O stretching vibration in alcohol (Figure 1c). The vibration for C−O−C and C−C−O are similar to those for CD (Figure 1d).

After tosylation of the CD-SPION OH groups, the product was reacted with NaN_3 to yield N_3-CD-SPIONs. The band for N_3-CD-SPIONs at 2106 cm^{-1} is assigned to N═N═N antisymmetric stretching vibration in azide (Figure 2a). Bands between 1190 and 1000 cm^{-1} derive from the C−O−C of ether in CD. Alkyne-FA shows a band at 2126 cm^{-1} due to C≡C stretching vibration in alkyne (Figure 2b). After reaction between FA-CD-SPIONs and alkyn-FA, a band appears at 1542 cm^{-1} attributed to 1,2,3-triazole (38). Neither the band for azide (2106 cm^{-1}) nor that for alkyne (2126 cm^{-1}) are observed for the product (Figure 2c), which demonstrates successful conversion of alkyne and azide groups to 1,2,3-triazole by the click reaction. There are also bands at 1700 cm^{-1} due to the C═O stretching vibration of carboxylic acid in FA and between 1190 and 1000 cm^{-1} due to the C−O−C stretching vibration of ether in CD, which demonstrate that FA binds chemically to CD by the click reaction. Bands at 584 and 433 cm^{-1} marked with solid triangles are due to the Fe−O in spinel, which demonstrates that FA and CD bind chemically to spinel particles. The amount of organics in the FA-CD-SPIONs is 22%, measured by weight loss from the TG curve.

Figure 3 shows XRD patterns for FA-CD-SPIONs, Fe_3O_4, and γ-Fe_2O_3. The FA-CD-SPIONs are shown to be crystalline, and the positions and relative intensities of all diffraction peaks are in good agreement with spinel iron oxide, Fe_3O_4, or γ-Fe_2O_3. The crystalline size is estimated to be 8.0 nm based on the Scherrer equation.

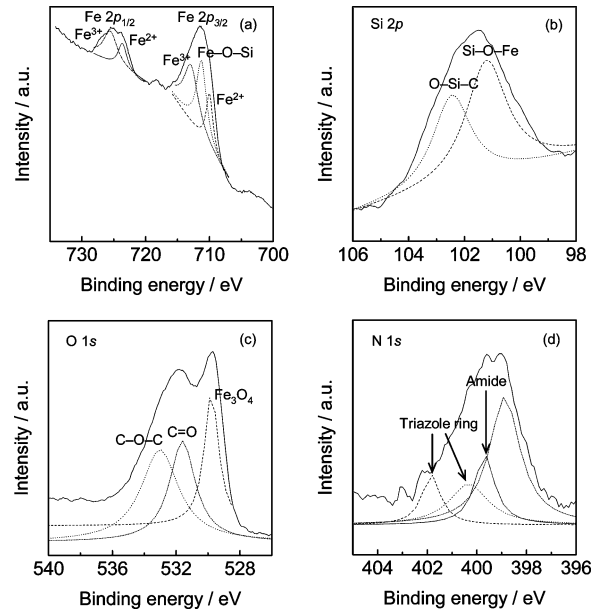

FIGURE 4. X-ray photoelectron spectra of FA-CD-SPIONs: (a) Fe 2p, (b) Si 2p, (c) O 1s, and (d) N 1s.

Figure 4 shows XPS spectra for FA-CD-SPIONs of Fe 2p, Si 2p, O 1s, and N 1s. Peaks for Fe 2$p_{1/2}$ and Fe 2$p_{3/2}$ are observed at 724.9 and 711.4 eV, respectively (Figure 4a), identical to those reported for bulk Fe_3O_4 (39). Bands for Fe 2$p_{3/2}$ and 2$p_{1/2}$ can be deconvoluted into three and two peaks at 710.1, 711.3, and 713.1 eV and 723.7 and 725.6 eV, respectively. Peaks at 710.1 and 723.7 eV are due to Fe^{2+} ions in the octahedral sites of Fe_3O_4, and those at 713.1 and 725.6 eV are due to Fe^{3+} ions in the tetrahedral and octahedral sites of Fe_3O_4 (39, 40). Hence, the SPIONs include Fe^{2+} ions in their lattices. Although a characteristic peak for γ-Fe_2O_3 is known to appear between 714 and 720 eV, it is not observed for Fe_3O_4; no such peak is observed for the FA-CD-SPIONs. Also, the peak at 711.3 eV is due to Fe−O−Si bonds (35). Additionally, peaks at 102.4 and 101.1 eV in Si 2p band are due to O−Si−C and Si−O−Fe, respectively (Figure 4b) (41). Therefore, the formation Fe−O−Si bonds is confirmed for FA-CD-SPIONs. The O 1s band can be deconvoluted into three peaks at 533.0, 531.6, and 529.9 eV (Figure 4c). The band at 533.0 eV is for bulk Fe_3O_4 (39). The bands at 531.6 and 529.9 eV can be assigned to the O of organic C−O−C and C═O species, respectively (42). The N 1s band is deconvoluted into four bands at 398.9, 399.8,

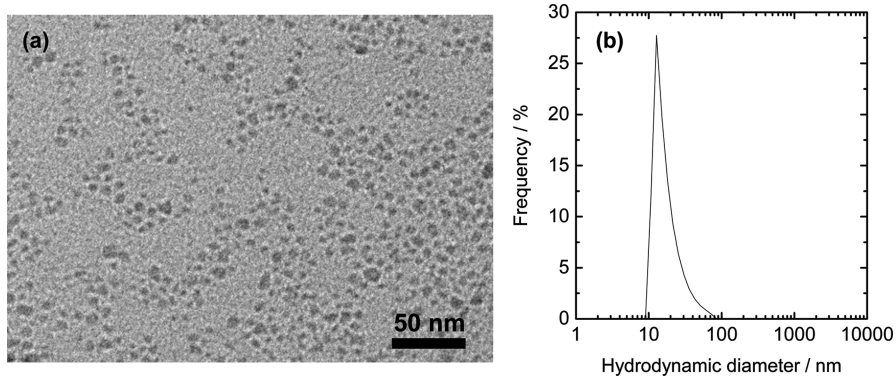

FIGURE 5. (a) TEM image of FA-CD-SPIONs. (b) Hydrodynamic diameter distribution of FA-CD-SPIONs by DLS measurement.

400.3, and 401.8 eV (Figure 4d). The bands at 399.8 and 398.9 eV are due to the amide N and other N of FA, respectively. The bands at 401.8 and 400.3 eV with an area ratio of 1/2 are in accordance with those of triazole ring N as reported (43). Thus, XPS results support the formation of Fe_3O_4 chemically bound with organic molecules by Fe−O−Si bonds.

Figure 5 shows the microstructure of the FA-CD-SPIONs and their particle size distribution. Particles are dispersed uniformly without aggregation. The mean size of inorganic particles is 8.2 ± 0.7 nm (relative standard deviation of 8.5%), in good agreement with the crystallite size estimated by XRD. Hydrodynamic diameter distribution in number measured by dynamic light scattering (DLS) shows a modal diameter of 12.4 nm with a polydispersity of 0.27 (Figure 5b). The modal diameter is larger than the mean size determined by TEM, because the organic molecules on the surface of the SPIONs swell in water. Thus, DLS revealed the whole size including organic phase in water, although TEM showed the size of inorganic phase in the dry state. TEM and DLS demonstrated that FA-CD-SPIONs formed no agglomerates above 100 nm. Because the enhanced permeability and retention (EPR) effect, or passive targeting, is applicable to NPs below 100 nm, the size of FA-CD-SPIONs is suitable for biomedical application (44).

Magnetic nanoparticles for medical applications should be hydrophilic and stable in water. The obtained FA-CD-SPIONs were dispersed in a mixture of water and chloroform (0.5 mg mL^{-1}) for examination of their hydrophilicity and stability in water. The aqueous phase exists above the oil phase of chloroform because of its lower density. The FA-CD-SPIONs disperse in water due to the hydrophilic CD and FA molecules on the surface, and are collectable by magnet (Figure 6a,b). The stability of FA-CD-SPIONs in water was evaluated by measuring the light transmittance of the aqueous phase immediately after dispersion and a month later (Figure 6c). There was no change in transmittance; this confirmed the good stability of FA-CD-SPIONs in water.

Magnetic Properties of FA-CD-SPIONs. For medical applications, it is important that SPIONs retain their favorable magnetic properties after functionalization with CD and FA. The saturation magnetization of FA-CD-SPIONs is 51 emu g^{-1} (Figure 7) and the corrected saturation magnetization is 65.4 emu g^{-1}, calculated on the basis of

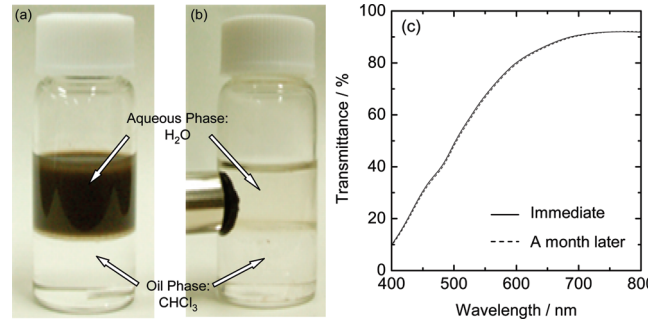

FIGURE 6. (a) Affinity test of FA-CD-SPIONs in water and chloroform. (b) Magnetically attracted FA-CD-SPIONs dispersed in water. (c) Stability test of FA-CD-SPIONs in water by measuring the light transmittance of the aqueous phase immediately after dispersion (solid line) and after 1 month (broken line).

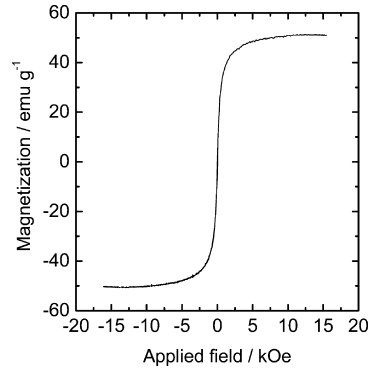

FIGURE 7. Magnetization vs applied field curve of FA-CD-SPIONs at room temperature.

the amounts of inorganic and organic phases of FA-CD-SPIONs from TG results; the former is 78 wt % and the latter is 22 wt %. The corrected value of 65.4 emu g^{-1} corresponds to 72% bulk Fe_3O_4 at room temperature (90 emu g^{-1}) (45). The magnetization curve shows neither remanence nor coercivity, implying that the nanoparticles are superparamagnetic, as demonstrated by the Langevin function (46)

$$M(H) = M_S\left(\coth\left(\frac{\mu H}{k_B T}\right) - \frac{k_B T}{\mu H}\right) \quad (1)$$

where M_S is the saturation magnetization, H is the applied magnetic field, k_B is Boltzmann's constant, T is the absolute temperature, and μ is the magnetic moment. Fitting eq 1 to

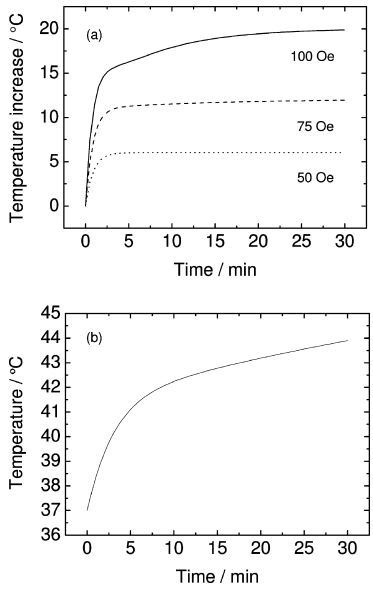

FIGURE 8. (a) Temperature increase of FA-CD-SPIONs powder stuffed into a Teflon tube with time under a HFMF with 230 kHz in frequency and 50−100 Oe in amplitude. (b) Temperature increase of the spherical agar phantom dispersed with 6 mg/mL of FA-CD-SPIONs under a HFMF with 230 kHz in frequency and 100 Oe in amplitude.

the magnetization data yields 1.3×10^{-17} J T^{-1} or 1.4×10^{6} μ_B of the magnetic moment for a FA-CD-SPIONs, where μ_B, the Bohr magneton, is 9.3×10^{-24} J T^{-1}. This demonstrates that FA-CD-SPIONs are superparamagnetic, because paramagnetic moments are generally only a few μ_B and, in contrast, superparamagnetic moments are as large as 1×10^{5} μ_B (47). Superparamagnetic properties of FA-CD-SPIONs are critical for their application in biomedical and bioengineering fields to prevent aggregation and enable rapid redispersal when the magnetic field is removed.

Hyperthermic Effect. Temperature increase (ΔT) under a HFMF was evaluated for FA-CD-SPIONs powder (5.8 mg) stuffed into a Teflon tube. Figure 8a shows a plot of ΔT with time under a 230 kHz AC magnetic field and 50, 75, and 100 Oe. Temperature increases upon application of a HFMF, and ΔT increases with increasing magnetic field strength; ΔT in 30 min at 50, 75, and 100 Oe are 6, 12, and 20 °C, respectively. These results demonstrate that the ΔT can be controlled by adjusting the strength of the magnetic field. Also, Ramanujan et al. reported that Fe_3O_4 particle/poly(N-isopropylacrylamide) composite, which contained 2.5 wt % of 3−5 μm Fe_3O_4 particles, produced the increase in temperature of 15 °C under 21 Oe and 375 kHz for 260 s (48). In this study, the increase in temperature of 15 °C was achieved under 100 Oe and 230 kHz for 230 s. Thus, the hyperthermic effect of FA-CD-SPIONs was comparable with that of the composite by Ramanujan et al. (48) The temperature increase stabilizes after 5 min for 50 and 75 Oe, whereas the temperature continues to increase for 20 min at a higher magnetic field of 100 Oe. The heat generation is considered to equilibrate with the heat dissipation to the outside of sample system, because the time required for stabilization at a higher magnetic field is longer than that at lower magnetic fields.

ΔT for a phantom was also measured under a HFMF of 230 kHz and 100 Oe (Figure 8b). FA-CD-SPIONs (6 mg mL^{-1}) were uniformly dispersed in the phantom. ΔT in 12 and 30 min are 5.5 and 7 °C, respectively. Considering that body temperature is 37 °C, the temperature after 12 min is optimal for hyperthermia treatment. The specific absorption rate (SAR), or denoted specific loss power, is defined as the power needed to heat 1 g of a magnetic material. The SAR is calculated according to the following equation (49)

$$\mathrm{SAR} = C\left(\frac{dT}{dt}\right)\left(\frac{M}{m}\right) \qquad (2)$$

where C is the specific heat capacity of the phantom (4.186 J g^{-1} K^{-1}), dT/dt is the initial slope of the temperature vs time curve when HFMF is applied, M is the total mass, namely the mass of phantom plus FA-CD-SPIONs, and m is the mass of the SPIONs. The SAR value calculated from eq 2 is 23 W g^{-1}. Because the SAR value is proportional to the square of the field strength and directly proportional to the frequency (50, 51), it needs to be normalized to 1 MHz and 100 Oe for comparison with the literature data (52). The normalized value is 100 W g^{-1}, comparable to literature data for variously sized ferrite particles in water; reported normalized values are 40 W g^{-1} (12 nm) by Drake et al. (52), 63 W g^{-1} (100−150 nm) by Brusentsov et al. (53), 12−56 W g^{-1} (7.5−416 nm) by Ma et al. (54), 0.5−104 W g^{-1} (6−8 nm) by Hergt et al. (55), and 77 W g^{-1} (10 nm) by Wang et al. (56) Particle cores with higher magnetization exhibit greater heating efficiency, enabling use of a lower particle concentration for hyperthermia.

Release of TMX from FA-CD-SPIONs. The release of hydrophobic drug, TMX, from FA-CD-SPIONs by external stimulus (direct heating or HFMF) was measured as described in the Experimental Section. TMX-loading efficiency is calculated according to the following equation

$$\text{loading efficiency} = m/M \times 100 \qquad (3)$$

where M is the mass of used TMX (20 mg) and m is the mass of the drug in the FA-CD-SPIONs (8.8 mg). The loading efficiency calculated from eq 3 is 44%. This indicates that TMX is easily included into the CDs on the surface of the SPIONs simply by impregnating TMX solution with the FA-CD-SPIONs. Also, Misra et al. reported that the drug-loading capacity of polyethyleneoxide-coated MNPs was ~50% (16). Thus, the loading efficiency in this study is comparable with that reported by Misra et al. The magnetization of the TMX-loaded FA-CD-SPIONs was 48.0 emu g^{-1}.

TMX-loaded FA-CD-SPIONs were dispersed in water at 45 °C. To investigate the amount of TMX released from the FA-CD-SPIONs, the FA-CD-SPIONs were collected by magnet at a regular time interval and the absorbance of the residual solution was measured by UV−vis spectrophotometry. Figure 9a shows the change in absorbance. Absorbance at 234 nm increases with dispersion time, indicating that TMX included in CD on the SPIONs is released by heating at 45 °C.

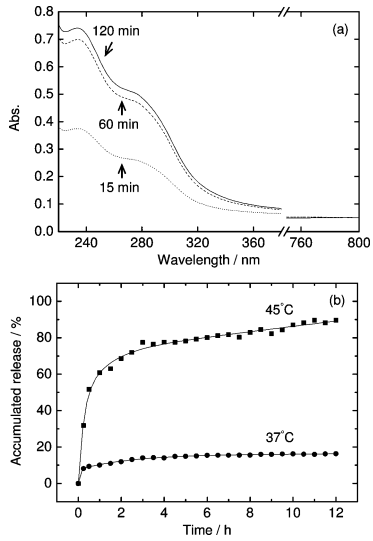

FIGURE 9. (a) UV−vis spectra of TMX solution released from FA-CD-SPIONs at 45 °C. (b) Release profiles of TMX from FA-CD-SPIONs at 37 and 45 °C.

Figure 9b shows the release profiles of TMX from the FA-CD-SPIONs in water at 37 and 45 °C without AC filed. The release rate of TMX at 45 °C is faster than that at 37 °C because higher temperature causes faster diffusion of TMX and weaker hydrophobic interactions between TMX and CD. In general, the rate of diffusion is given by the following equation (57):

$$\frac{W_0 - W_t}{W_0} = kt^n \qquad (4)$$

where W_0 and W_t are the masses of TMX-loaded FA-CD-SPIONs at the onset of release and after a given time, respectively, k is the release rate constant, t is the release time, and n is the diffusion exponent. The n value is related to the release mechanism; a value of 0.45 indicates Fickian release (57). The n values for 37 and 45 °C from eq 4 are 0.12 and 0.40, respectively. Both values are less than 0.45, because hydrophobic interactions between TMX and CD retard the release of TMX to below that for Fickian release. The temperature-dependent nature of the interactions results in a lower n value at 37 °C than that at 45 °C.

Figure 10 shows the temperature increase of water and controlled release of TMX from the FA-CD-SPIONs triggered by on−off switching of the HFMF of 230 kHz and 100 Oe. The temperature of water containing TMX-loaded FA-CD-SPIONs (20 mg mL^{-1}) increases up to 42.5 °C, which is the optimum temperature for hyperthermia, immediately after application of the field as shown in Figure 10a. The concentration of FA-CD-SPIONs (20 mg mL^{-1}) is one-sixth that used for the magnetic hyperthermia of tumor cells in rats (58). The SAR value is 132 W g^{-1} from eq 2 where M is the mass of water plus TMX-loaded FA-CD-SPIONs (5.1 g). Hyperthermic effect by application of the HFMF acts as a driving force for release of TMX from CD on the SPIONs (Figure 10c). Release continues during application of the field and stops upon removal of the field. Thus, the controlled release of

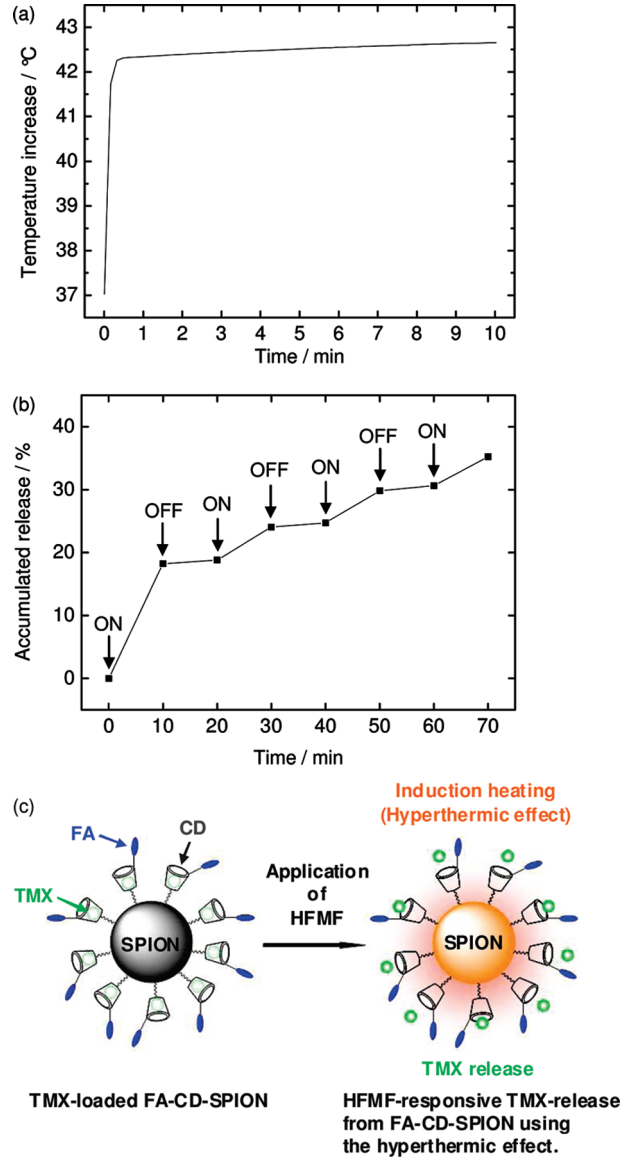

FIGURE 10. (a) The temperature increase of the water dispersed with 20 mg/mL of TMX-loaded FA-CD-SPIONs under a HFMF with 230 kHz in frequency and 100 Oe in amplitude. (b) Controlled release of TMX from FA-CD-SPIONs by switching a HFMF on and off. (c) Schematic illustration of TMX release from FA-CD-SPIONs using the hyperthermic effect by applying a HFMF.

payloads using FA-CD-SPIONs allows drug delivery at a remote location. Furthermore, the heat for drug release can be used for hyperthermia treatment and enhancement of drug effect.

The amount of TMX released from the FA-CD-SPIONs was 0.54 mg (540 mg mL^{-1}). When 10 mg m^{-2} TMX were administered orally to a woman patient twice a day, the TMX concentration in the blood was 150 ng mL^{-1} (59). Thus, the amount of TMX released was sufficient to have an adverse effect on the cancer cells. Because the amount of TMX loaded on the SPIONs can be decreased easily by decreasing the inclusion amount to CD, this is a merit of the FA-CD-SPIONs.

Figure 11 shows the viability of microglial cells after incubation in a medium containing FA-CD-SPIONs from 1 to 100 μg mL^{-1} for 0.5 to 24 h. As shown in Figure 11, the

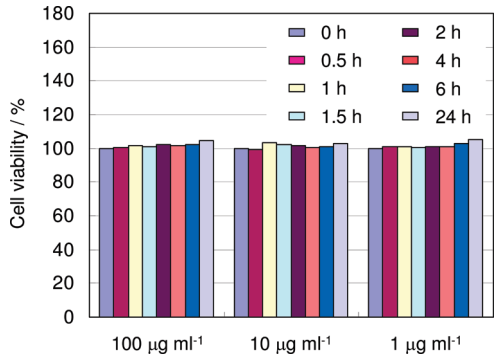

FIGURE 11. Cytotoxicity profiles of FA-CD-SPIONs at concentrations from 1 to 100 μg mL^{-1} for various incubation times.

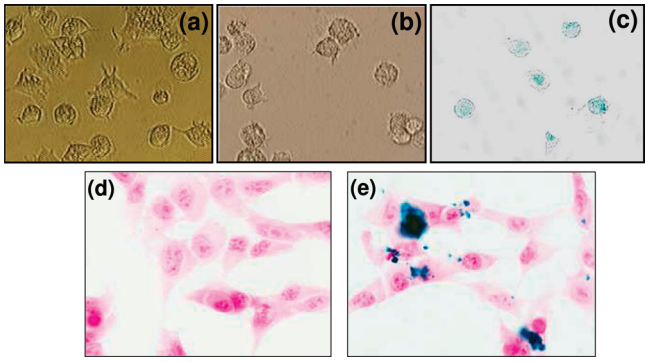

FIGURE 12. Optical microscopic images: (a) microglial cells (control), (b) microglial cells after incubation with FA-CD-SPIONs for 1 h, (c) microglial cells corresponding to b stained with Berlin blue, (d) glioma cells stained with nuclear fast red (control), (e) glioma cell after incubation with FA-CD-SPIONs for 1 h stained with Berlin blue.

cell viability after 24 h was slightly higher than that before incubation in the concentration range. Thus, the SPIONs were noncytotoxic for the cells.

Figure 12 shows the optical microscopic images of the cells before and after incubation of microglia and glioma cells with FA-CD-SPIONs for 1 h. After incubation with microglial cell, the agglomeration of the SPIONs is not observed outside the cells (Figure 12b). Figure 12c shows that the stained SPIONs with Berlin blue do not remain on the cell surfaces, but are incorporated within the cells. Glioma cells shown in Figure 12d are stained with nuclear fast red. FA-CD-SPIONs stained with Berlin blue are internalized by the glioma cells as shown in Figure 12e. Thus, the functionalization with organic molecules enhances the cellular affinity of SPIONs to allow entry into the cells. The phagocytosis by mocrophages in the body prevents the SPIONs to reach the tumor cells. However, Johannsen et al. reported that 81.6% magnetic particles remained in the tumor cells, after 10 days of the administration to the cells of rats (58). Hence, not all SPIONs are considered to be uptaken by macrophages in vivo, as the FA-CD-SPIONs has a smaller size than that reported (58). Further modifications of FA-CD-SPIONs with suitable molecules like polyethylene glycol are required to avoid phagocytosis by macrophage.

4. CONCLUSION

FA and CD were successfully immobilized on the surface of SPIONs to provide hydrophilia and long-term stability in water. FA-CD-SPIONs were monodisperse and superparamagnetic. They generated heat under HFMF and their hyperthermic properties were controllable by the adjustment of field strength. Furthermore, they loaded TMX simply by mixing of the former and the latter in water because of inclusion property of CD. The release control of TMX was accomplished by on−off switching HFMF; TMX-release continued during the application of HFMF through the hyperthermic effect of the SPIONs and stopped upon removal of the HFMF. The heat for drug release can be useful for hyperthermia treatment and the enhancement of drug effects.The FA-CD-SPIONs were confirmed to be nontoxic for normal cells by cytotoxity assay.

REFERENCES AND NOTES

(1) Mornet, S.; Vasseur, S.; Grasset, F.; Duguet, E. *J. Mater. Chem.* **2004**, *14*, 2161.
(2) Gao, J.; Gu, H.; Xu, B. *Acc. Chem. Res.* **2009**, *42*, 1097.
(3) Laurent, S.; Forge, D.; Port, M.; Roch, A.; Robic, C.; Elst, L. V.; Muller, R. N. *Chem. Rev.* **2008**, *108*, 2064.
(4) Arruebo, M.; Fernández-Pacheco, R.; Ibarra, M. R.; Santamaria, J. *Nano Today* **2007**, *2*, 22.
(5) Kim, J.; Piao, Y.; Hyeon, T. *Chem. Soc. Rev.* **2009**, *38*, 372.
(6) Kim, J.; Lee, J. E.; Lee, S. H.; Yu, J. H.; Lee, J. H.; Park, T. G.; Hyeon, T. *Adv. Mater.* **2008**, *20*, 478.
(7) Wang, B.; Xu, C.; Xie, J.; Yang, Z.; Sun, S. *J. Am. Chem. Soc.* **2008**, *130*, 14436.
(8) Misra, R. D. K. *Mater. Sci. Technol.* **2008**, *24*, 1011.
(9) Zhang, J. L.; Srivastava, R. S.; Misra, R. D. K. *Langmuir* **2007**, *23*, 6342.
(10) Zhang, J.; Misra, R. D. K. *Acta Biomater.* **2007**, *3*, 838.
(11) Yuan, Q.; Venkatasubramanian, R.; Hein, S.; Misra, R. D. K. *Acta Biomater.* **2008**, *4*, 1024.
(12) Purushotham, S.; Ramanujan, R. V. *Acta Biomater.* **2010**, *6*, 502.
(13) Purushotham, S.; Chang, P. E. J.; Rumpel, H.; Kee, I. H. C.; Ng, R. T. H.; Chow, P. K. H.; Tan, C. K.; Ramanujan, R. V. *Nanotechnology* **2009**, *20*, 305101.
(14) Ang, K. L.; Venkatraman, S.; Ramanujan, R. V. *Mater. Sci. Eng., C* **2007**, *C27*, 347.
(15) Zhang, J.; Rana, S.; Srivastava, R. S.; Misra, R. D. K. *Acta Biomater.* **2008**, *4*, 40.
(16) Rana, S.; Gallo, A.; Srivastava, R. S.; Misra, R. D. K. *Acta Biomater.* **2007**, *3*, 233.
(17) Gu, H.; Xu, K.; Yang, Z.; Chang, C. K.; Xu, B. *Chem. Commun.* **2005**, 4720.
(18) Liu, T.-Y.; Liu, K.-H.; Liu, D.-M.; Chen, S.-Y.; Chen, I.-W. *Adv. Funct. Mater.* **2009**, *19*, 616.
(19) Hu, S.-H.; Chen, S.-Y.; Liu, D.-M.; Hsiao, C.-S. *Adv. Mater.* **2008**, *20*, 2690.
(20) Liu, T.-Y.; Hu, S.-H.; Liu, K.-H.; Shaiu, R.-S.; Liu, D.-M.; Chen, S.-Y. *Langmuir* **2008**, *24*, 13306.
(21) Uekama, K.; Hirayama, F.; Irie, T. *Chem. Rev.* **1998**, *98*, 2045.
(22) Hirayama, F.; Uekama, K. *Adv. Drug. Deliv. Rev.* **1999**, *36*, 125.
(23) Sudimack, J.; Lee, R. J. *Adv. Drug Delivery Rev.* **2000**, *41*, 147.
(24) Almadori, G.; Bussu, F.; Navarra, P.; Galli, J.; Paludetti, G.; Giardina, B.; Maurizi, M. *Cancer* **2006**, *107*, 328.
(25) Weitman, S. D.; Lark, R. H.; Coney, L. R.; Fort, D. W.; Frasca, V.; Zurawski, V. J.; Kamen, B. A. *Cancer Res.* **1992**, *52*, 3396.
(26) Deng, Y.; Hou, Z.; Wang, L.; Cherian, C.; Wu, J.; Gangjee, A.; Matherly, L. H. *Mol. Pharmacol.* **2008**, *73*, 1274.
(27) Kohler, N.; Fryxell, G. E.; Zhang, M. *J. Am. Chem. Soc.* **2004**, *126*, 7206.
(28) Hayashi, K.; Moriya, M.; Sakamoto, W.; Yogo, T. *Chem. Mater.* **2009**, *21*, 1318.
(29) Tayim, H. A.; Sabri, M. *Inorg. Nucl. Chem. Lett.* **1973**, *9*, 753.
(30) Hayashi, K.; Shimizu, T.; Asano, H.; Sakamoto, W.; Yogo, T. *J. Mater. Res.* **2008**, *23*, 3415.
(31) Khan, A. R.; Forgo, P.; Stine, K. J.; D'Souza, V. T. *Chem. Rev.* **1998**, *98*, 1977.
(32) Ha, K.; Lee, Y.-J.; Lee, H. J.; Yoon, K. B. *Adv. Mater.* **2000**, *12*, 1114.

(33) Kolb, H. C.; Finn, M. G.; Sharpless, K. B. *Angew. Chem., Int. Ed.* **2001**, *40*, 2004.
(34) Sawada, M.; Imai, F.; Suzuki, H.; Hayakawa, M.; Kanno, T.; Nagatsu, T. *FEBS Lett.* **1998**, *433*, 37.
(35) Silverstein, R. M.; Webster, F. X.; Kiemle, D. J. *Spectrometric Identification of Organic Compounds*, 7th ed; John Wiley & Sons: New York, 2005; pp 72.
(36) Scheidegger, A.; Borkovec, M.; Sticher, H. *Geoderma* **1993**, *58*, 43.
(37) Ishii, M.; Nakahira, M.; Yamanaka, T. *Solid State Commun.* **1972**, *11*, 209.
(38) Billes, F.; Endrédi, H.; Keresztury, G. *J. Mol. Struct.* **2000**, *530*, 183.
(39) Mills, P.; Sullivan, J. L. *J. Phys. D: Appl. Phys.* **1983**, *16*, 723.
(40) Fujii, T.; Groot, F. M. F.; Sawatzky, G. A.; Voogt, F. C.; Hibma, T.; Okada, K. *Phys. Rev. B* **1999**, *59*, 3195.
(41) Choi, W. K.; Ong, T. Y.; Tan, L. S.; Loh, F. C.; Tan, K. L. *J. Appl. Phys.* **1998**, *83*, 4968.
(42) Ikeo, N.; Iijima, Y.; Niimura, N.; Sigematsu, M.; Tazawa, T.; Matsumoto, S.; Kojima, K.; Nagasawa, Y. *Handbook of X-ray Photoelectron Spectroscopy*: Japan Electro-Optic Laboratory: Tokyo, 1991; Chapter 5.
(43) Ciampi, S.; Böcking, T.; Kilian, K. A.; James, M.; Harper, J. B.; Gooding, J. J. *Langmuir* **2007**, *23*, 9320.
(44) Nie, S.; Xing, Y.; Kim, G. J.; Simons, J. W. *Annu. Rev. Biomed. Eng.* **2007**, *9*, 257.
(45) Liu, X.; Kaminski, M. D.; Guan, Y.; Chen, H.; Liu, H.; Rosengart, A. J. *J. Magn. Magn. Mater.* **2006**, *306*, 248.
(46) Morrish, A. H. *The Physical Principles of Magnetism*; JohnWiley & Sons: New York, 1965.
(47) Dennis, C. L.; Borges, R. P.; Buda, L. D.; Ebels, U.; Gregg, J. F.; Hehn, M.; Jouguelet, E.; Ounadjela, K.; Petej, I.; Prejbeanu, I. L.; Thornton, M. J. *J. Phys.: Condens. Matter.* **2002**, *14*, R1175.
(48) Ramanujan, R. V.; Ang, K. L.; Venkatraman, S. *J. Mater. Sci.* **2009**, *44*, 1381.
(49) Latham, A. H.; Williams, M. E. *Acc. Chem. Res.* **2008**, *41*, 411.
(50) Rosensweig, R. E. *J. Magn. Magn. Mater.* **2002**, *252*, 370.
(51) Lao, L. L.; Ramanujan, R. V. *J. Mater. Sci.-Mater. Med.* **2004**, *15*, 1061.
(52) Drake, P.; Cho, H. J.; Shih, P. S.; Kao, C. H.; Lee, K. F.; Kuo, C. H.; Lin, X. Z.; Lin, Y. J. *J. Mater.Chem.* **2007**, *17*, 4914.
(53) Brusentsov, N. A.; Gogosov, V. V.; Brusentsova, T. N.; Sergeev, A. V.; Jurchenko, N. Y.; Kuznetsov, A. A.; Kuznetsov, O. A.; Shumakov, L. I. *J. Magn. Magn. Mater.* **2001**, *225*, 113.
(54) Ma, M.; Wu, Y.; Zhou, J.; Sun, Y.; Zhang, Y.; Gu, N. *J. Magn. Magn. Mater.* **2004**, *268*, 33.
(55) Hergt, R.; Andrä, W.; d'Ambly, C. G.; Hilger, I.; Kaiser, W. A.; Richter, U.; Schmidt, H. G. *IEEE. Trans. Magn.* **1998**, *34*, 3745.
(56) Wang, X.; Gu, H.; Yang, Z. *J. Magn. Magn. Mater.* **2005**, *293*, 334.
(57) Ritger, P. L.; Peppas, N. A. *J. Controlled Release* **1987**, *5*, 37.
(58) Johannsen, M.; Thiesen, B.; Jordan, A.; Taymoorian, K.; Gneveckow, U.; Waldöfner, N.; Scholz, R.; Koch, M.; Lein, M.; Jung, K.; Loening, S. A. *Prostate* **2005**, *64*, 283.
(59) Fabian, C.; Sternson, L.; El-Serafi, M.; Cain, L.; Hearne, E. *Cancer* **1981**, *48*, 876.

AM100237P